JCTC Journal of Chemical Theory and Computation

Article

pubs.acs.org/JCTC

On the Computation of Adiabatic Energies in Aza-Boron-Dipyrromethene Dyes

Siwar Chibani,[†] Boris Le Guennic,*[,‡] Azzam Charaf-Eddin,[†] Olivier Maury,[§] Chantal Andraud,[§] and Denis Jacquemin*[,†]

[†]Laboratoire CEISAM—CNRS 6230, Université de Nantes, 2 Rue de la Houssinière, BP 92208, 44322 Nantes Cedex 3, France

[‡]Institut des Sciences Chimiques de Rennes, Université de Rennes 1, CNRS 6226, 35042 Rennes Cedex, France

[§]Laboratoire de Chimie, Université Lyon 1, Ecole Normale Supérieure de Lyon, CNRS 5182, 46 allée d'Italie, 69364 Lyon, France

Supporting Information

ABSTRACT: We have simulated the optical properties of Aza-Boron-dipyrromethene (Aza-BODIPY) dyes and, more precisely, the 0−0 energies as well as the shape of both absorption and fluorescence bands, thanks to the computation of vibronic couplings. To this end, time-dependent density functional theory (TD-DFT) calculations have been carried out with a systematic account of both vibrational and solvent effects. In a first step, we assessed different atomic basis sets, a panel of global and range-separated hybrid functionals as well as different solvent models (linear-response, corrected linear-response, and state-specific). In this way, we have defined an accurate yet efficient protocol for these dyes. In a second stage, several simulations have been carried out to investigate acidochromic and complexation effects, as well as the impact of side groups on the topology of the optical bands. In each case, theory is able to accurately reproduce experimental results and the proposed protocol is consequently useful to design new dyes featuring improved properties.

1. INTRODUCTION

The near-infrared spectral range (NIR 700−1600 nm) is of particular interest because it includes two transparency domains where the light is less absorbed or scattered: (i) the "biological window" between 700−1100 nm corresponding to the transparency domain of living tissues giving the opportunity of noninvasive deep penetration of the biological tissues, at the origin of numerous applications in biology and medicine,[1] and (ii) the "telecommunication window" at 1300 and 1550 nm corresponding to the transparency domain of silica optical fiber at the basis of the actual telecommunication network.[2,3] These particular properties of the NIR spectral range have triggered this past decade the development of dyes featuring absorption, emission, or nonlinear optical properties in this region for applications ranging from material science (laser and telecommunication materials) to biology (imaging, sensing, and therapy). Many excellent reviews on this topic are available in the literature.[4−9]

Among the various NIR chromophores, boron-dipyrromethene (BODIPY) and its nitrogenated parent, namely aza-boron-dipyrromethene (Aza-BODIPY), nowadays concentrate tremendous efforts due to their remarkable photophysical properties.[10,11] Indeed, these monomethine cyanine analogues present improved photostability, large absorption coefficients, and fluorescent quantum yields as well as tunable fluorescence wavelengths. Recent applications of these dyes can be found in photovoltaics,[12,13] advanced optoelectronics,[14−16] nonlinear optics,[17−19] bioimaging or sensing,[20−23] and photodynamic therapy.[24−26] Consequently, several studies focused on the development of new (Aza-)BODIPY dyes with red-shifted photophysical properties, conserving high luminescence quantum yield efficiency in the NIR range. To reach this goal, various approaches have been proposed taking advantage of the (i) peripheral functionalization with electron-donating groups,[27−29] (ii) rigidification of rotatable moieties,[30−35] and (iii) extension[36−39] or planarization[40−44] of the π-path.

Theoretical models able to deliver insights into the properties of electronically excited states are a useful source of information to complement experimental measurements. However, due to the size of the Aza-BODIPY structures, one needs to make compromise between the desired accuracy and the computational burden. In that framework, density functional theory (DFT), and more precisely its time-dependent form (TD-DFT),[45,46] is the ab initio method of choice, as it may treat structures containing up to ca. 300 atoms, at least within the vertical approximation. In fact, TD-DFT is the most widely used tool to model optical spectra of organic molecules in gas-phase, solution, or even in more complex environmental conditions.[47−57] For the specific case of Aza-BODIPY derivatives, several dedicated (TD-)DFT works have been published previously.[18,39,41,42,58−60] However, at one notable exception,[44,61] they all relied on the crude highest occupied molecular orbital−lowest unoccupied molecular orbital (HOMO−LUMO) picture or use the vertical TD approximation to model absorption (that is single-point TD-DFT calculations are performed on the ground-state geometry, ignoring completely the structure of the excited-state). These approaches cannot be viewed as completely satisfying strategies for Aza-BODIPY. Indeed, irrespective of the selected functional, vertical TD-DFT does not allow a systematically accurate prediction of the longest wavelength of maximal

Received: July 20, 2012
Published: August 9, 2012

absorption (λ_{max}) for this specific family.[42,58,60] For instance, Gresser et al. computed, with the B3LYP/6-31+G(d,p) approach, positions of the bands that can be up to 100 nm off their experimental value, and more importantly, at the same level of theory, the auxochromic effects are only very qualitatively reproduced.[42] Likewise, in our previous investigation,[60] we proposed a computational strategy that allowed reproduction of the absorption wavelengths for Aza-BODIPY characterized by a significant through-space charge-transfer (CT), but the results remained rather poor for the cyanine-like bands, that are also hallmarks of these dyes. Recently, Truhlar and co-workers, using Monte Carlo results of Send et al.[62] as benchmarks, have shown that the large TD-DFT errors commonly reported for cyanine derivatives can be (at least partly) ascribed to the failure of the vertical TD approximation used to obtain absorption energies, rather than to the actual weaknesses of recent DFT functionals.[63] Therefore, there is a hope to improve the theoretical description of the optical properties of Aza-BODIPY derivatives by simulating their excited-state in a more complete way. For that reason, in the present investigation, we have performed, for the first time, benchmarks for the 0−0 energies of Aza-BODIPY considering both vibrational and solvent effects with a panel of functionals and basis sets. We have also modeled the shape of the absorption band of Aza-BODIPY, thanks to the computation of Franck−Condon factors, a task never tackled previously for these derivatives. This allows us to propose a rational protocol (*the good answer for the good reason*) to compute the 0−0 energies with a sufficient accuracy, subsequently paving the way toward a more rational design of new structures with tailored properties.

This paper is organized as follows: in section 2, we outline the applied computational procedures; in section 3, we present the results of TD-DFT benchmarks (basis set, functional and solvent model); in section 4, we present applications of our methodology to interesting chemical cases (complexation, acidochromism, vibronic shapes...). Eventually, we conclude and provide an outlook of future research directions.

2. METHODOLOGY

All our calculations were carried out with the Gaussian09 program,[64] tightening both self-consistent field (10^{-9} a.u.) and geometry optimization (10^{-5} a.u.) convergence thresholds. The spectroscopic properties were simulated as follows. The ground-state (S_0) geometrical parameters have been determined with DFT and the nature of the stationary points (minima) was confirmed by a subsequent vibrational frequency analysis. Within the vertical approximation, the energies of the electronically excited-states have been calculated with TD-DFT on the S_0 geometries. In Aza-BODIPY, the lowest-lying singlet excited-state, S_1, is strongly dipole-allowed and corresponds to the most intense absorption band in the visible part of the experimental spectra. The $S_0 \rightarrow S_1$ transition energies computed on the ground-state geometries will be referred to as E^{vert-a} (vertical absorption) in the following. The geometries of the S_1 states have been determined using analytical TD-DFT gradients implemented in Gaussian09.[65,66] The vertical transition energies calculated on the optimal S_1 geometries correspond to the vertical emission energies, E^{vert-f} (vertical fluorescence). The vibrational signatures of the excited-states were subsequently determined by numerical differentiation of the TD-DFT gradients. This allowed us not only to ascertain the absence of imaginary frequencies and to compute the zero point vibrational energies (ZPVE) of the S_1 states but also to determine vibronic couplings (see below). The adiabatic energies, E^{adia}, can be calculated as the difference between the S_1 and S_0 electronic energies determined at their respective optimal geometries. Eventually, E^{0-0} have been obtained by subtracting the difference of ZPVE between the two states, ΔE^{ZPVE}, from the adiabatic energies. The interested reader may find extra details in ref 67. For the records, our calculations have been performed within the C_2 point group when possible, in order to lighten the computational burden. In the same way, we have replaced long side alkyl chains used in the experiments by methyl groups (e.g., $NHex_2$ was changed to NMe_2), as it is expected that the length of the alkyl chains has no significant impact on the optical properties. We have also applied the default (fine) integration grid, except when a convergence problem appeared. In these cases, we used the tighter (ultrafine) integration grid. Of course, the same integration grid was systematically used for both S_0 and S_1 states.

In this work, we wish to first define an efficient TD-DFT protocol and the selected functional is subsequently a key parameter. For this reason, we considered a set of six functionals: B3LYP,[68,69] the most widely used global hybrid, PBE0,[70,71] that has been shown to be successful for evaluating λ_{max},[72,73] BMK,[74] that was identified as the most adequate method for reproducing the vertical absorption energies of Aza-BODIPY presenting a strong CT character,[60] M06-2X,[75] that is successful for cyanines,[63] as well as CAM-B3LYP[76] and ωB97X-D,[77] two range-separated hybrids providing accurate description of the electronically excited-states of organic dyes.[55,78−81] Four split-valence atomic basis sets have also been used: 6-31G(d), 6-311+G(d), 6-311G(2d,p), and 6-311+G(2d,p), the two latter respectively providing converged structural and electronic parameters in Aza-BODIPY dyes.[60]

The solvent effects have been accounted for with the polarizable continuum model (PCM).[82] The selected solvents are acetonitrile (ACN), chloroform ($CHCl_3$), dichloromethane (DCM), and toluene (Tol). While for ground-state features, the computation of environmental effects within the PCM approach is rather univocal, the calculation of excited-state properties may be performed with several schemes. First, let us distinguish the equilibrium (eq) and the nonequilibrium (neq) limits. In the former, the solvent is fully relaxed with respect to the excited-state density of the solute, an approach adequate to optimize the S_1 structures and to compute the related vibrational spectra. The equilibrium limit is also the model adapted to the determination of E^{adia} and E^{0-0}, two energies that correspond to fully relaxed S_0 and S_1 states. In the latter neq limit, only the electrons of the solvent do adapt to the new electronic configuration of the solute, a scheme dedicated to the modeling of absorption and fluorescence (vertical) transition energies. For absorption (emission), the neq/eq distinction applies to the S_1 (S_0) state. In other words, the neq and eq fluorescence wavelengths reported in the following differ by the model used to calculate the S_0 energy at the S_1 geometry. Second, three PCM approaches are available in Gaussian09 for computing the solvent reaction field surrounding the electronically excited states: the simplest linear-response (LR),[50,83] the only available approximation for TD-DFT geometry optimization and vibrational calculations, the corrected linear response (cLR),[84] and the state-specific (SS) models.[85] The two latter models allow to evaluate the polarization of the cavity when the dye is in the S_1 state, thanks to pertubative (cLR) or self-consistent (SS) procedures. Therefore, they provide more

Scheme 1. Representation of the Series of Compounds Investigated Herein (Training and Test Steps)[a]

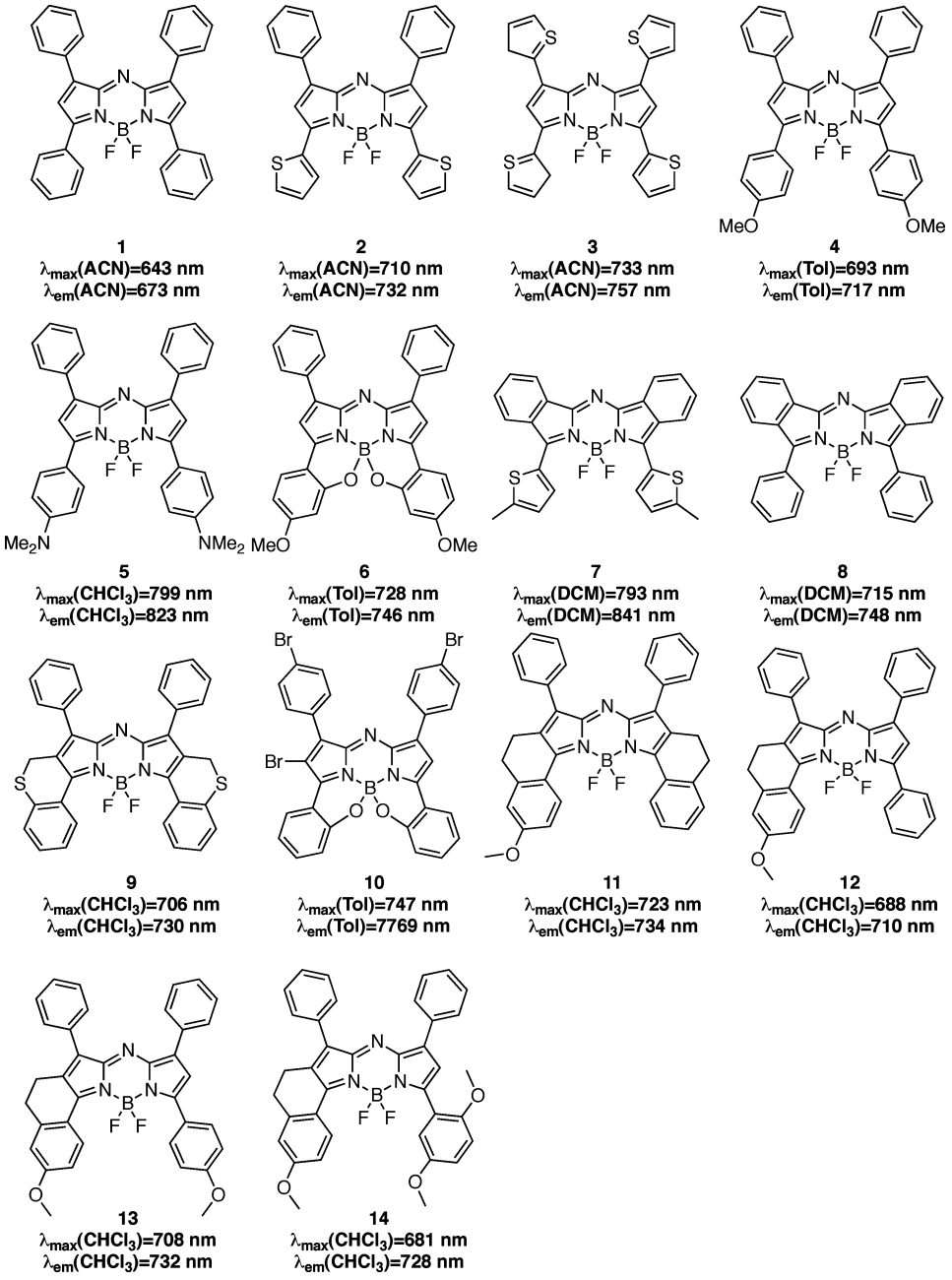

[a]The experimental values are also reported and are from refs 44 (**1**–**3**), 29 (**4**), 28 (**5**), 31 (**6** and **10**), 41 (**7** and **8**), 30 (**9**–**14**).

Table 1. Basis Set Effects on the Optical Properties of Dye 3, Using the PCM(ACN)-TD-DFT Approach with the PBE0 Functional[a]

basis sets		E^{vert-a}		E^{vert-f}	E^{adia}	ΔE^{ZPVE}	E^{0-0}
geometry	energy	(LR,neq)	(LR,eq)	(LR,eq)	(LR,eq)	(LR,eq)	(LR,eq)
6-31G(d)	6-31G(d)	1.852	1.623	1.472	1.547	−0.047	1.500
	6-311+G(d)	1.805	1.572	1.420	1.503	*−0.047*	1.456
	6-311G(2d,p)	1.818	1.587	1.436	1.521	*−0.047*	1.474
	6-311+G(2d,p)	1.798	1.567	1.415	1.499	*−0.047*	1.452
6-311+G(d)	6-311+G(d)	1.812	1.575	1.423	1.502	−0.048	1.454
6-311G(2d,p)	6-311G(2d,p)	1.833	1.598	1.445	1.521	−0.043	1.477
	6-311+G(2d,p)	1.812	1.578	1.424	1.494	*−0.043*	1.451

[a]Values in italics have been computed with the basis set used for geometry optimization. Complementary results are given in the SI. All values are in electronvolts.

dx.doi.org/10.1021/ct300618j | J. Chem. Theory Comput. 2012, 8, 3303−3313

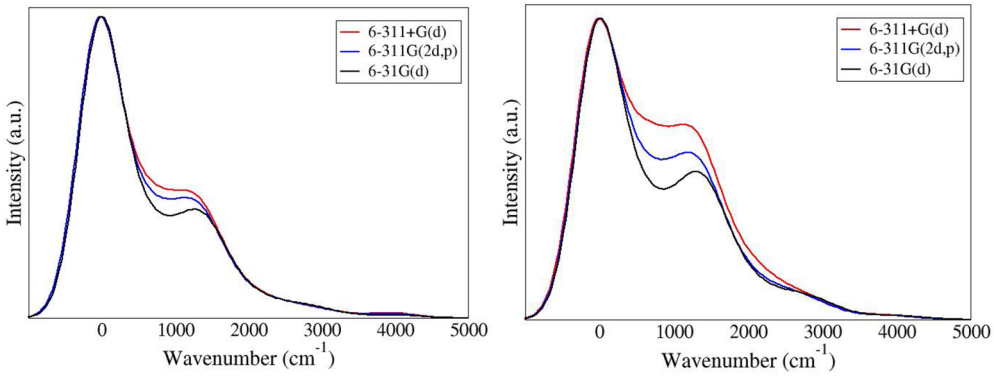

Figure 1. Impact of the atomic basis set on the vibronic shapes for dye **3** with PCM-PBE0 (left) and PCM-CAM-B3LYP (right) levels. Results have been normalized for the main absorption band.

Table 2. Computed Solvent Effects for Dyes 1 (ACN), 2 (ACN), 3 (ACN), 4 (Toluene), and 5 ($CHCl_3$), Using a Series of Solvent Models[a]

	E^{vert-a}						
dye	gas	(LR,eq)	(cLR,eq)	(SS,eq)	(LR,neq)	(cLR,neq)	(SS,neq)
1	2.239	1.904	2.227	2.220	2.117	2.229	2.224
2	2.099	1.717	2.076	2.064	1.954	2.080	2.071
3	1.994	1.623	1.972	1.959	1.852	1.974	1.963
4	2.118	1.949	2.098	2.075	1.958	2.098	2.077
5	1.917	1.611	1.809	1.700	1.707	1.822	1.734

	E^{vert-f}				ΔE^{ZPVE}	
dye	gas	(LR,eq)	(SS,eq)	(SS,neq)	gas	(LR,eq)
1	2.032	1.694	2.014	2.013	−0.068	−0.051
2	1.955	1.575	1.936	1.935	−0.068	−0.048
3	1.837	1.472	1.814	1.813	−0.064	−0.047
4	1.965	1.795	1.934	1.933	−0.061	−0.051
5	1.818	1.514	1.635	1.627	−0.060	−0.039

	E^{adia}			E^{0-0}		
dye	gas	(LR,eq)	(SS,eq)	Gas	(LR,eq)	(SS,eq)[b]
1	2.137	1.798	2.118	2.068	1.747	2.067
2	2.028	1.645	2.006	1.960	1.597	1.958
3	1.916	1.547	1.890	1.852	1.500	1.843
4	2.042	1.871	2.010	1.981	1.820	1.959
5	1.867	1.562	1.683	1.807	1.523	1.644

[a]All results are with the PBE0/6-31G(d) approach. cLR and SS energies have been determined on LR geometries. Data for other functionals is available in the SI. [b]Determined using the (LR,eq) ZPVE correction and the (SS,eq) adiabatic energies.

accurate excited-state energies than the LR scheme, but at the price of a significant increase of the computational cost.

Vibrationally resolved spectra within the harmonic approximation were computed using the FCclasses program.[86−88] The reported spectra have been simulated at 298 K using a convoluting Gaussian function presenting a half width at half-maximum (HWHM) that has been adjusted to allow meaningful comparisons with experiments (typical value: 0.04 eV). A maximal number of 25 overtones for each mode and 20 combination bands on each pair of modes were included in the calculation. The maximum number of integrals to be computed for each class was set to 10^6.

3. BENCHMARKS

3.1. Basis Set Effects. We have evaluated the basis set effects on the three first dyes represented in Scheme 1. These systems have been investigated experimentally by Gresser et al.[42] and Zhang et al.[44] Vertical B3LYP/6-31+G(d,p) absorption and B3LYP/TZVP absorption/emission results may also be found in these two previous works. The PBE0 data for **3** are collated in Table 1 and have been obtained with the LR-PCM approach. The PBE0 values of **1** and **2** as well as the corresponding CAM-B3LYP data are listed in the Supporting Information (SI). The ZPVE correction, by far the most expensive contribution in terms of computational requirements, is rather small for the tested dyes (−0.051 eV at most). Indeed, the typical values for ΔE^{ZPVE} ranges from −0.03 to −0.15 eV in small and medium-size molecules.[55,67,89] More importantly, while ΔE^{ZPVE} is significantly smaller with the range-separated hybrid than with its global counterpart (see the SI), the basis set effects remain trifling. Indeed, the typical variations between the three tested atomic basis set are on the order of 0.005 eV. Therefore one could estimate the ΔE^{ZPVE} with the smallest basis set, 6-31G(d), at the only price of a very slight overestimation of the actual values. For the optical properties, the 6-311+G(2d,p)//6-311G(2d,p) [Energy//Geometry] combination may be used as reference, as it yields

converged structures and transition energies.[60] It is obvious from Table 1 that the 6-31G(d) basis set overestimates E^{vert-a}, E^{vert-f}, E^{adia}, and E^{0-0} by ca. 0.050 eV. However, single point 6-311+G(2d,p) calculations performed on 6-31G(d) structures are sufficient to correct the largest part of the error. Such approach provides vertical transition energies within 0.020 eV of the reference, and the 0−0 energies are even more accurate. Indeed, for the latter, the errors are rather negligible 0.008, 0.000, and 0.001 eV, for dyes **1**, **2**, and **3**, respectively (see Table 1 and SI). It is therefore reasonable to determine the geometrical parameters at the 6-31G(d) level and to compute the transition energies thanks to (vertical) calculations performed with larger basis set(s). This procedure, already advocated by Grimme and co-workers,[55,90] will be used in the following applying a 6-311+G(2d,p) basis set to determine the energies. Figure 1 provides the vibronic shapes computed with three basis sets. As can be seen, both functionals foresee a significant shoulder to the main band (see section 4), but the shapes are very similar for the three basis sets (PBE0), or only slightly modified by the extension of the basis set (CAM-B3LYP), confirming that 6-31G(d) provides sufficiently accurate geometrical and vibrational parameters for our purposes.

3.2. Solvent Models. In Table 2, we present PBE0/6-31G(d) transition energies obtained with a panel of solvent models and compare them to gas phase results. The results obtained with five other functionals are available in the SI. We have selected the three same dyes as in Table 1 but have added dyes **4** (in an apolar solvent) and **5** (in a polar medium), that present a significant CT character in order to have a more diverse panel. It turns out that the LR-PCM model is rather unsatisfying for this class of dyes. Indeed, for E^{0-0}, the difference between the (LR,eq) and (SS,eq) results ranges from −0.361 (**2**) to −0.121 eV (**5**). Quite interestingly, the gas phase and SS results are alike for Aza-BODIPY with a cyanine like transition (**1**, **2**, and **3**). However, this relationship does not hold for **5**, for which the (SS,eq)-gas difference attains −0.183 eV. Clearly, one should include solvent effects and go beyond the LR model to reach accurate results. It is also noteworthy that the ΔE^{ZPVE} is significantly smaller in PCM than in gas-phase, the impact of solvation being about three times larger than the effect of the basis set. If one turns toward the absorption, one notices clearly that the pertubative cLR model, that is more computationally effective than its self-consistent SS counterpart, is extremely efficient for the first four dyes, but becomes less pertinent for the CT dye **5**: it is therefore a valid alternative for investigating cyanine-like transitions. As for the basis set effects, there is a strong parallelism between the impact of the solvent on the vertical and adiabatic results, e.g. the SS-LR difference on E^{0-0} are 0.320, 0.361, 0.343, 0.139, and 0.121 eV going down the column in Table 2 and the corresponding E^{vert-f} (E^{vert-a}) variations are 0.320 (0.316), 0.361 (0.347), 0.342 (0.336), 0.139 (0.126), and 0.121 (0.089) eV, respectively. Clearly, this means that the solvent effects do not significantly tune the geometrical reorganization energies of both the ground and excited states. Eventually, let us note that the nonequilibrium effects are relatively small in the SS model, irrespective of the investigated phenomena. The fact that neq effects tends to be larger in LR-PCM than in other PCM models is consistent with a recent benchmark work.[67]

For **5**, we have performed the same PCM calculations but with the 6-311+G(2d,p) basis set. For E^{vert-a}, the neq LR, cLR, and SS energies are 1.662, 1.778, and 1.695 eV, respectively. That is the cLR and SS models bring corrections of +0.116 and +0.033 eV, respectively, that are very similar to the values obtained with the 6-31G(d) basis set: +0.115 and +0.027 eV. Likewise, for the fluorescence, the (LR,eq), (SS,eq), and (SS,neq) 6-311+G(2d,p) values are 1.168, 1.594, and 1.587 eV, respectively, corresponding to successive corrections of +0.126 and −0.007 eV, once again completely in the line of the 6-31G(d) data of +0.121 and −0.008 eV. The same relationship holds for the adiabatic energies,[91] clearly suggesting that one could rely on

$$E^{adia}(SS, eq) = E^{S_1//S_1}_{6\text{-}31G(d)//6\text{-}31G(d)}(SS, eq) - E^{S_0//S_0}_{6\text{-}31G(d)//6\text{-}31G(d)}(eq) + \Delta E^{adia-BS} \quad (1)$$

where,

$$\Delta E^{adia-BS} = E^{adia}_{6\text{-}311+G(2d,p)//6\text{-}31G(d)}(LR, eq) - E^{adia}_{6\text{-}31G(d)//6\text{-}31G(d)}(LR, eq) \quad (2)$$

for computing the adiabatic energies. Compared to the more "exact",

$$E^{adia}(SS, eq) = E^{S_1//S_1}_{6\text{-}311+G(2d,p)//6\text{-}31G(d)}(SS, eq) - E^{S_0//S_0}_{6\text{-}311+G(2d,p)//6\text{-}31G(d)}(eq) \quad (3)$$

the selection of eq 1 allows us to lighten the computational effort by removing the SS computation with the largest basis set. For the first seven dyes of Scheme 1, using the six functionals, we have compared the results obtained through these two procedures. It turned out that the average absolute deviation is as small as 0.004 eV, whereas the maximal discrepancy does not exceed 0.009 eV (a full list of results can be found in the SI). We have therefore decided to proceed solely with the former procedure in the following.

3.3. Functionals. We can now provide best estimates (BE) for the 0−0 energies, by adding the adiabatic energies of eq 1 to the ZPVE correction,

$$E^{0-0}(BE, eq) = E^{adia}(SS, eq) + \Delta E^{ZPVE}_{6\text{-}31G(d)}(LR, eq) \quad (4)$$

This equation allows us to reach sound estimates of the 0−0 energies, but the results cannot be directly compared to experimental measurements. Indeed, the commonly accepted 0−0 reference is the meeting point between normalized absorption and emission curves (AFCP: absorption/fluorescence crossing point).[55,67] However, this point corresponds to a nonequilibrium phenomena and is strictly speaking, not the 0−0 energy. To account for the neq effects, we have applied a further correction,

$$E^{AFCP}(BE, neq) = E^{0-0}(BE, eq) + \frac{1}{2}[\Delta E^{vert-a}_{6\text{-}31G(d)} + \Delta E^{vert-f}_{6\text{-}31G(d)}] \quad (5)$$

where the two corrections simply reads

$$\Delta E^{vert-a} = E^{vert-a}(SS, neq) - E^{vert-a}(SS, eq) \quad (6)$$

$$\Delta E^{vert-f} = E^{vert-f}(SS, neq) - E^{vert-f}(SS, eq) \quad (7)$$

We redirect the interest reader to ref 67 for a justification of the one-half factor as well as discussions about this methodology. For the present set of molecules, the corrections brought by

Table 3. Theoretical Best Estimates Obtained for the Absorption/Fluorescence Crossing Point, Equation 5[a]

dye	B3LYP	PBE0	BMK	M06-2X	CAM-B3LYP	ωB97X-D
1	1.992	2.031	2.122	2.096	2.114	2.159
2	1.873	1.908	2.005	1.923	1.953	1.937
3	1.748	1.796	1.914	1.848	1.857	1.871
4	1.892	1.930	2.032	2.002	2.016	2.036
5	1.577	1.622	1.713	1.750	1.790	1.841
6	1.852	1.883	1.923	1.946	1.937	1.927
7	1.690	1.725	1.708	1.776	1.779	1.808
8	1.920	1.954	1.953	1.988	1.998	2.024
9	1.799	1.863	1.973	2.011	2.011	2.051
MSE	−0.129	−0.170	−0.240	−0.240	−0.252	−0.275
MAE	0.129	0.170	0.240	0.240	0.252	0.275
rms	0.139	0.176	0.242	0.242	0.254	0.278
R	0.90	0.92	0.98	0.95	0.96	0.92

[a]All values are in electronvolts. At the bottom of the table, one can find the computed mean signed (MSE), absolute (MAE), and root-mean (RMS) errors compared to experiment. *R* is the linear correlation coefficient obtained by comparing theoretical and experimental data (see Scheme 1).

ΔE^{vert-a} and ΔE^{vert-f} are rather small (if not negligible), as can be deduced from the data of Table 2. The results obtained from eq 5 for the nine symmetric dyes of Scheme 1 are collected in Table 3. These nine Aza-BODIPY offers a representative panel of the possible chemical substitution existing in the field (see the Introduction). The mean signed errors (MSE) listed in Table 3 indicate that the theoretical transition energies are systematically too large, which is in the line of what has been found within the LR-PCM vertical approach.[60] The obtained absolute deviation (MAE) range from 0.13 to 0.28 eV, depending on the functional, is within the expected TD-DFT accuracy (ca. 0.25 eV) for the E^{AFCP} of organic fluorophores.[67] This further confirms that, by going beyond the vertical approximation, one can reasonably estimate the excited-state energies of cyanine-like transitions.[63] The smallest average deviations are provided by B3LYP which is very close to the experimental spot (rms of 0.14 eV). However, this quantitative success is at the price of less consistent estimates (poorer *R*): the variations of the optical properties induced by chemical substitutions are satisfactorily but not accurately reproduced. BMK circumvents the problem (see Figure 2), with an impressive (*R*) and is therefore more adequate for designing new molecules. Consequently, we have applied only the B3LYP and BMK functionals in the following.

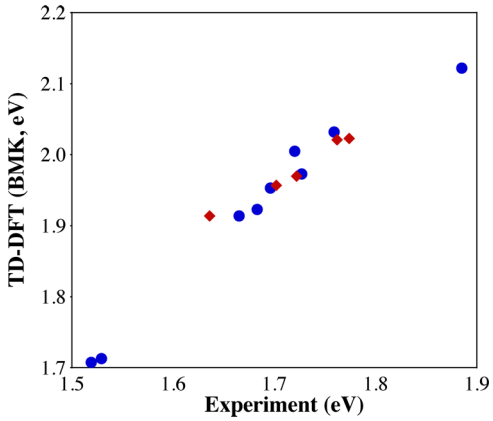

Figure 2. Comparison between BMK and experimental AFCP for symmetric, **1**−**9** (blue circles), and asymmetric, **10**−**14** (red diamonds), dyes. All values are in electronvolts.

4. APPLICATIONS

4.1. Asymmetric Dyes. To assess the validity of our model, we have used a test set composed of dyes **10**−**14** (see Scheme 1), that are part of conformationally restricted structures presenting large quantum yields.[30,31] This set is not a simple extension of our training list of molecules as they are asymmetric, e.g. **12**−**14** are only hindered on one side, making the excited-state asymmetric. The results obtained with both the B3LYP and the BMK hybrid functionals are collected in Table 4, whereas the BMK results have also been represented in Figure 2. As can be seen, these asymmetric structures are evaluated with a similar accuracy as their symmetric counterparts. Indeed, we obtain an MSE and an rms of −0.258 and 0.258 eV for the **10**−**14** subset, respectively, completely in the line of the results of Table 3. Likewise, the *R* determined for the full set (**1**−**14**) is 0.98, that is the same as the one obtained on the symmetric structure subset. This is a further proof of the reliability of our computational approach.

Table 4. Theoretical Best Estimates Obtained for the AFCP through Equation 5[a]

dye	B3LYP	BMK
10	1.813	1.914
11	1.895	1.957
12	1.946	2.023
13	1.869	1.970
14	*b*	2.021

[a]All values are in electronvolts. See the title of Table 3 for more details. [b]SS calculations fail to properly converge, making calculations on an equal footing impossible.

4.2. Auxochrome Impact on Band Shapes. For the three first dyes of Scheme 1, one can find a comparison between experimental and theoretical (PCM-TD-BMK) band shapes in Figure 3. As discussed above, the SS 0−0 energies are too large with this functional, and hence, the computed wavelengths are too small compared to experiment. However, the impact of the replacement of the phenyl rings by thiophene groups is reproduced in a very satisfying way. Indeed, not only the bathochromic shifts of both absorption and emission peaks when going from **1** to **2** and next from **2** to **3** are well restored by TD-DFT, but in addition, the ab initio band shapes are

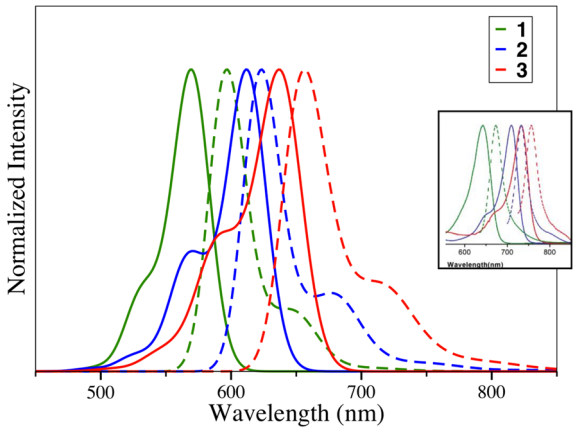

Figure 3. Theory−experiment comparisons for dyes **1**, **2**, and **3**. BMK was used (B3LYP data available in the SI): (full lines) absorption, (dashed lines) fluorescence. The experimental inset on the right is reprinted with permission from ref 44. Copyright 2012 American Chemical Society.

accurate. Indeed, for absorption, one notes the presence of a shoulder at small wavelength in the experimental spectra,[44] this shoulder being higher in **2** and **3** than in **1**. This effect is nicely reproduced by TD-DFT, though the height of the shoulder is overestimated by ca. 20% by BMK (this error is slightly mitigated by B3LYP, see the SI). Likewise, the emission bands present experimentally less structure than their absorption counterparts but extend to longer wavelengths for all dyes.[44] This trend is also given by the applied model, though, the height of the shoulder is again slightly overrated. We have investigated the nature of the vibrational couplings playing a role in these shoulders. However, we found that they could not be explained by one or two isolated modes but result from the combination of a large number of vibrational transitions, making chemically intuitive interpretations impossible.

4.3. Complexation Effects. Of course, one of the major applications of fluorophores is their ion sensing ability. Recently, it has been shown that the interaction between a specific aza-BODIPY dye presenting pyridine rings and mercury ions is strong enough to allow the optical detection of the latter.[20] The complexation clearly implies lone pairs of the three nitrogen atoms and the metallic cation (see top of Scheme 2). Here, we have simulated the optical properties of this system, using the same basis set combination as above but applying the LanL2DZ basis set and pseudopotential for Hg^{2+}. It turns out that the most stable conformer for the free fluorophore, **15(a)**, differs from the complexation isomer by the orientation of the two top pyridine rings. Nevertheless, the energetic differences between the three **15** isomers of Scheme 2 remain quite small. Indeed, PCM-BMK/6-31G(d) calculations provide relative ground-state energies of 0.00, 1.75, and 4.78 kcal·mol^{-1} for **15(a)**, **15(b)**, and **15(c)**, respectively. These values are small compared to the estimated Hg^{2+} complexation energy of ca. 247.9 kcal·mol^{-1},[92] indicating that the interaction with the dication largely overcomes the cost of the rotation of the pyridine rings. Therefore, in the following, we only considered **15(a)** and **15(Hg^{2+})**. The charge-transfer distance, as measured

Scheme 2. (Top) Conformers and Complexation of Compound 15 (See Ref 20 for Experimental Data); (Middle) Illustration of the Acidochromism Effects for 5 (See Ref 28 for Experimental Data); (Bottom) New Dyes with Predicted near-IR Absorption Energies

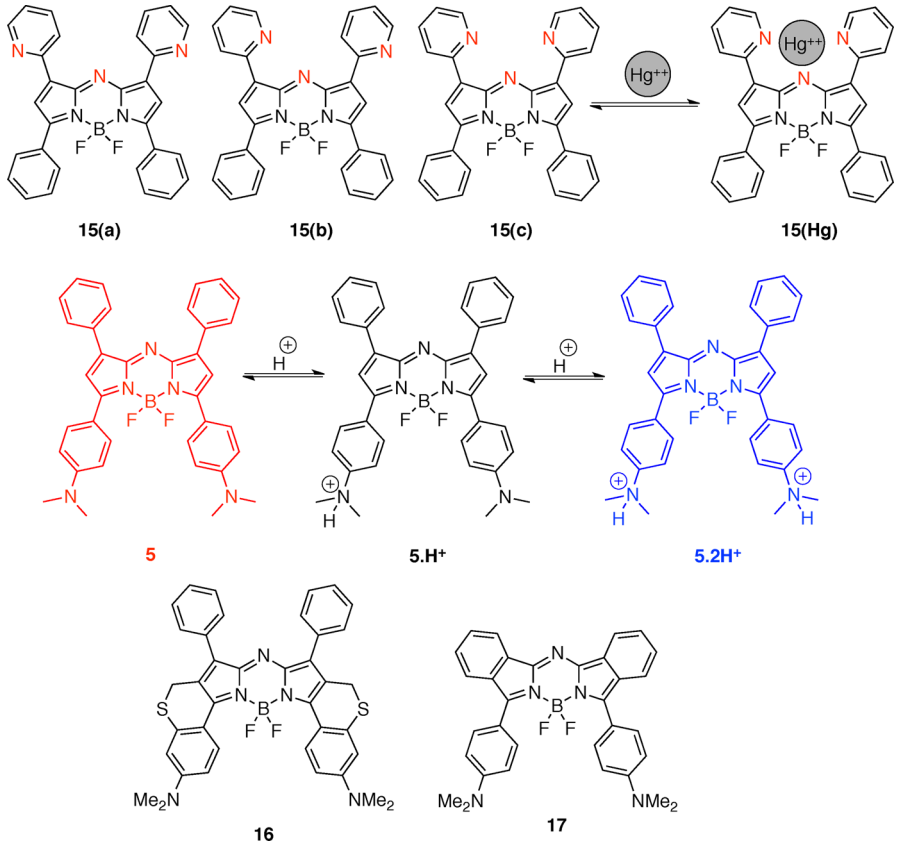

dx.doi.org/10.1021/ct300618j | J. Chem. Theory Comput. 2012, 8, 3303−3313

by the separation between the barycenters of the electron density gain/depletion zones,[93,94] attain 1.11 and 1.74 Å, for these two compounds, respectively (BMK results). This small improvement of the charge-transfer hints for a bathochromic shift upon complexation that is observed.[20] Indeed, the experimental AFCP point goes from 1.855 to 1.761 eV in acetonitrile upon Hg^{2+} binding, both the absorption and emission bands undergoing a ca. +35 nm (−0.090 eV) shift. Blindly applying eq 5 provides qualitatively incorrect corrections, the estimated shifts being very far from the measurements: +0.175 eV (B3LYP) and +0.156 eV (BMK).[95] This is certainly a deceiving result, especially when the simpler E^{vert-a}(LR,neq) approximation provides an estimate of −0.090 eV (BMK), that is on the experimental spot. An analysis of the individual contributions to the theoretical E^{AFCP}(BE,neq) reveals that the SS correction is unrealistic for **15**(Hg^{2+}), illustrating the difficulty to reach a physically sound excited-state polarization of the PCM cavity for a dicationic derivative. Experimentally, the counterions are perchlorate anions, and we have therefore optimized the corresponding **15**(Hg^{2+})−(ClO_4^-)$_2$ aggregate. As can be seen in Figure 4, the ground

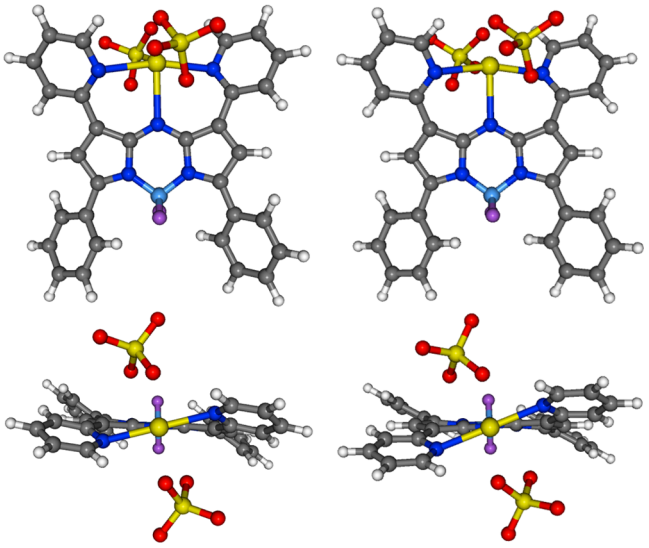

Figure 4. Front and top view of the **15**(Hg^{2+})−perchlorate complexes obtained at the PCM-BMK level of theory. The ground- and excited-state minimal structures are found on the left- and right-hand sides, respectively.

and excited-state minima are similar, though one notices a small contraction of −0.06 Å for the Hg^{2+}−N(BODIPY) distance. With this improved chemical model, our standard procedure, namely eq 5, provides a variation of −0.141 eV (BMK)[96] between **15**(**a**) and **15**(Hg^{2+}), which correctly restores the experimental evolution.

4.4. Acidochromism. The optical signatures of aza-BODIPY **5** are known to be very sensitive to the pH.[28] Indeed, while the neutral form displays an experimental AFCP point at 1.529 eV, this value attains 1.662 eV for the monoprotonated derivative and 1.892 eV for the diprotonated form (see center of Scheme 2).[28] This corresponds to successive increase of +0.133 and +0.230 eV of the transition energies. Qualitatively, these acidochromic shifts can be explained by investigating the reorganization of the electronic cloud induced by the absorption (Figure 5). For **5**, one notes a clear charge-transfer character from the dimethylamino

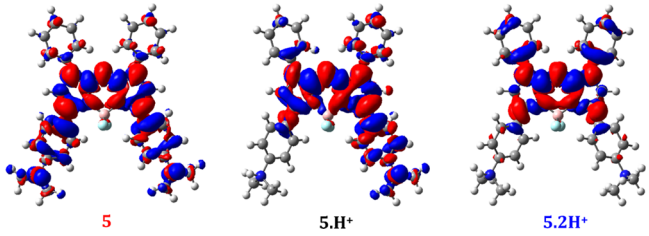

Figure 5. PCM-BMK/6-311+G(2d,p) electron density difference plots for neutral, cationic and dicationic **5**. The blue zones indicate electron density loss upon transition (donor) whereas the red zones correspond to increase of electron density upon transition (acceptors).

moieties toward the aza-BODIPY core, the top phenyl rings presenting only trifling contributions. The charge-transfer distance, computed with the above-mentioned approach,[93,94] attains 2.55 Å for **5**. Upon the first protonation, the CT character remains but is localized on one of the two arms, the protonated moiety being optically inactive. Eventually, for **5.2H**$^+$, the two *p*-NMe_2H^+−Ph groups do not play any significant role in the optical transition, which is mainly localized on the chromogenic center. Nevertheless, one notices a small CT character from the top phenyl rings to the aza-BODIPY center (CT distance of 1.17 Å). With B3LYP (BMK), the AFCP points are estimated to be at 1.577 (1.713), 1.761 (1.937), and 2.033 (2.210) eV, for **5**, **5.H**$^+$ and **5.2H**$^+$, respectively. This corresponds to successive increase of the transition energies of +0.184 (+0.224) and +0.272 (+0.273) eV. The first being overestimated compared to experiment, whereas the second is sufficiently accurate. In Figure 6, we compare

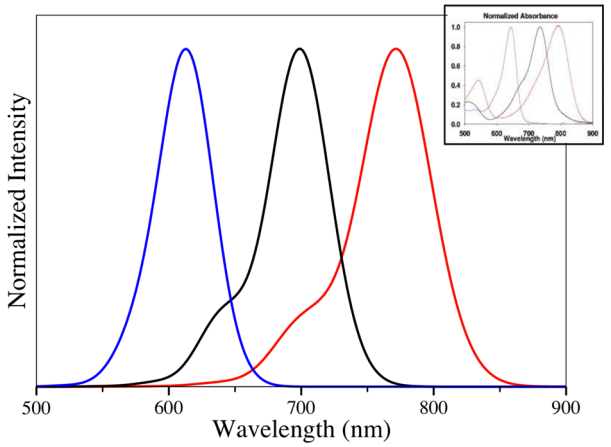

Figure 6. BMK−experiment comparison for the absorption bands of the three dyes of Figure 5: **5** (red), **5.H**$^+$ (black), and **5.2H**$^+$ (blue). The experimental inset on top right is reprinted with permission from ref 28. Copyright 2006 American Chemical Society.

experimental and theoretical absorption spectra. In the measurements, the absorption band is tighter for **5.2H**$^+$ than for both **5** and **5.H**$^+$, an effect that PCM-TD-BMK vibronic simulations reproduce in a very satisfying way. On the contrary, B3LYP does not give a reasonable estimate of the band shape for the **5.H**$^+$ structure: it provides a band topology similar to **5.2H**$^+$ rather than **5**, as in the measurements (see the SI).

Eventually, though in these cases, the cationic sites are distant from the chromogenic centers (see Figure 5); we have also simulated the AFCP of **5.H**$^+$ and **5.2H**$^+$ explicitly including the counterions (trifluoro-carboxylate, TFA, as in the experi-

ment).[28] The optimized structures may be found in the SI. With BMK, the predicted AFCP point are 1.909 and 2.150 eV for $\mathbf{5.H^+}$ and $\mathbf{5.2H^+}$, respectively.[96] This corresponds to successive acidochromic shifts of +0.196 and +0.241 eV, which are closer from experiment than the simulations without TFA.

5. CONCLUSIONS AND OUTLOOK

Using modern PCM-TD-DFT approaches, we have defined an efficient protocol to evaluate the spectral properties of Aza-BODIPY dyes. This computationally efficient procedure relies on a systematic calculation of state-specific solvation effects as well as the determination of the vibrational signatures of both the ground and excited-states. Using the BMK functional, that was already found effective within the vertical TD-DFT approximation, the evolution of the theoretical 0−0 energies are very consistent with the experimental trends but suffers from an almost constant deviation of ca. 0.25 eV. This systematic error can be reduced with B3LYP but at the price of a poorer, though still acceptable, correlation with experimental measurements. For dye design, we therefore clearly advocate the selection of the BMK hybrid as this functional also yields very accurate topologies of both the absorption and fluorescence bands. We have successfully applied our model to the investigation of asymmetrically substituted chromogens, pH-sensitive dyes as well as complexation effects. In each case, the proposed approach is both qualitatively and quantitatively consistent with experiment if the counterions used experimentally are explicitly included in the chemical model for formally charged compounds.

We are currently applying our protocol to the investigation of larger Aza-BODIPY dyes possessing strong CT character. In that framework, we have already simulated the AFCP of two new dyes (see bottom of Scheme 2) that combine two strong donor groups to stiffened (**16**) or extended (**17**) chromophoric cores. The obtained results are 1.614 eV (1.651 eV) with B3LYP and 1.638 eV (1.789 eV) with BMK, for **16** and **17**, respectively. Using the latter hybrid functional, one notices that only **16** yields a significant bathochromic shift compared to its "parents" (**5** and **9**), whereas **17** does not provide AFCP closer to the IR region than **5**. This illustrates how the developed protocol might be useful in guiding the experiments toward the most promising structures.

■ ASSOCIATED CONTENT

Supporting Information

Basis set investigation with the PBE0 and the CAM-B3LYP functionals. Solvent effects on the absorption, fluorescence, and adiabatic energies computed for all functionals. Comparison between gas phase and PCM vibronic shapes for **3**. Results obtained through eqs 1 and 3 for dyes **1**−**7**. B3LYP band shapes for dyes **1**−**3** as well as both the neutral and the charged **5** structures. Representation of $\mathbf{5.H^+}$ and $\mathbf{5.2H^+}$ with TFA counterions. This material is available free of charge via the Internet at http://pubs.acs.org/.

■ AUTHOR INFORMATION

Corresponding Author

*E-mail: boris.leguennic@univ-rennes1.fr (B.L.G.); Denis.Jacquemin@univ-nantes.fr (D.J.).

Notes

The authors declare no competing financial interest.

■ ACKNOWLEDGMENTS

S.C. and A.C.-E. thank the European Research Council (ERC, Marches 278845) for their Ph.D. and postdoctoral grants, respectively. D.J. acknowledges the European Research Council (ERC) and the *Région des Pays de la Loire* for financial support in the framework of a Starting Grant (Marches 278845) and a *recrutement sur poste stratégique*, respectively. This research used resources of (1) the GENCI-CINES/IDRIS (Grants c2012085117), (2) CCIPL (*Centre de Calcul Intensif des Pays de Loire*), and (3) a local Troy cluster.

■ REFERENCES

(1) Frangioni, J. V. *Curr. Opin. Chem. Biol.* **2003**, *7*, 626−634.
(2) Humbach, O.; Fabian, H.; Grzesik, U.; Haken, U.; Heitmann, W. *J. Non-Cryst. Solids* **1996**, *203*, 19−26.
(3) Harrisson, M. T.; Kershaw, S. V.; Burt, M. G.; Rogach, A. L.; Kornowski, A.; Eychmüller, A.; Weller, H. *Pure Appl. Chem.* **2000**, *72*, 295−307.
(4) Fabian, J.; Nakazumi, H.; Matsuoka, M. *Chem. Rev.* **1992**, *92*, 1197−1226.
(5) Mishra, A.; Behera, R. K.; Behera, P. K.; Mishra, B. K.; Behera, G. B. *Chem. Rev.* **2000**, *100*, 1973−2012.
(6) Kiyose, K.; Kojima, H.; Nagano, T. *Chem. Asian J.* **2008**, *3*, 506−515.
(7) Kulinich, A. V.; Ishchenko, A. A. *Russ. Chem. Rev.* **2009**, *78*, 141−162.
(8) Qian, G.; Wang, Z. Y. *Chem. Asian J.* **2010**, *5*, 1006−1029.
(9) Pansare, V. J.; Hejazi, S.; Faenza, W. J.; Prud'homme, R. K. *Chem. Mater.* **2012**, *24*, 812−827.
(10) Loudet, A.; Burgess, K. *Chem. Rev.* **2007**, *107*, 4891−4932.
(11) Ulrich, G.; Ziessel, R.; Harriman, A. *Angew. Chem., Int. Ed.* **2008**, *47*, 1184−1201.
(12) Erten-Ela, S.; Yilmaz, M. D.; Icli, B.; Dede, Y.; Icli, S.; Akkaya, E. U. *Org. Lett.* **2008**, *10*, 3299−3302.
(13) Rousseau, T.; Cravino, A.; Bura, T.; Ulrich, G.; Ziessel, R.; Roncali, J. *Chem. Commun.* **2009**, 1673−1675.
(14) Whited, M. T.; Djurovich, P. I.; Roberts, S. T.; Durrell, A. C.; Schlenker, C. W.; Bradforth, S. E.; Thompson, M. E. *J. Am. Chem. Soc.* **2011**, *133*, 88−96.
(15) Flavin, K.; Lawrence, K.; Bartelmess, J.; Tasior, M.; Navio, C.; Bittencourt, C.; O'Shea, D. F.; Guldi, D. M.; Giordani, S. *ACS Nano* **2011**, *5*, 1198−1206.
(16) Lehl, J.; Nierengarten, J.-F.; Harriman, A.; Bura, T.; Ziessel, R. *J. Am. Chem. Soc.* **2012**, *134*, 988−998.
(17) Zheng, Q.; Xu, G.; Prasad, P. *Chem.—Eur. J.* **2008**, *14*, 5812−5819.
(18) Bouit, P.-A.; Kamada, K.; Feneyrou, P.; Berginc, G.; Toupet, L.; Maury, O.; Andraud, C. *Adv. Mater.* **2009**, *21*, 1151−1154.
(19) Didier, P.; Ulrich, G.; Mély, Y.; Ziessel, R. *Org. Biomol. Chem.* **2009**, *7*, 3639−3642.
(20) Coskun, A.; Yilmaz, M.; Akkaya, E. U. *Org. Lett.* **2007**, *9*, 607−609.
(21) Murtagh, J.; Frimannsson, D. O.; OShea, D. F. *Org. Lett.* **2009**, *11*, 5386−5389.
(22) Han, J.; Loudet, A.; Barhoumi, R.; Burghardt, R. C.; Burgess, K. *J. Am. Chem. Soc.* **2009**, *131*, 1642−1643.
(23) Shi, W.-J.; Liu, J.-Y.; Ng, D. K. P. *Chem. Asian J.* **2012**, *7*, 196−200.
(24) Killoran, J.; Allen, L.; Gallagher, J.; Gallagher, W.; O'Shea, D. *Chem. Commun.* **2002**, 1862−1863.
(25) Byrne, A. T.; O'Connor, A. E.; Hall, M.; Murtagh, J.; O'Neill, K.; Curran, K. M.; Mongrain, K.; Rousseau, J. A.; Lecomte, R.; McGee, S.; Callanan, J. J.; O'Shea, D. F.; Gallagher, W. M. *Br. J. Cancer.* **2009**, *101*, 1565−1573.
(26) Adarsh, N.; Avirah, R. R.; Ramaiah, D. *Org. Lett.* **2010**, *12*, 5720−5723.

(27) Rurack, K.; Kollmannsberger, M.; Daub, J. *Angew. Chem., Int. Ed.* **2001**, *40*, 385−387.
(28) McDonnell, S. O.; O'Shea, D. F. *Org. Lett.* **2006**, *8*, 3493−3496.
(29) Loudet, A.; Bandichhor, R.; Wu, L.; Burgess, K. *Tetrahedron* **2008**, *64*, 3642−3654.
(30) Zhao, W. L.; Carreira, E. M. *Chem.—Eur. J.* **2006**, *12*, 7254−7263.
(31) Loudet, A.; Bandichhor, R.; Burgess, K.; Palma, A.; McDonnell, S. O.; Hall, M. J.; O'Shea, D. F. *Org. Lett.* **2008**, *10*, 4771−4774.
(32) Donyagina, V.; Shimizu, S.; Kobayashi, N.; Lukyanets, E. A. *Tetrahderon Lett.* **2008**, *48*, 6152−6154.
(33) Umezawa, K.; Nakamura, A.; Makino, H.; Citterio, D.; Suzuki, K. *J. Am. Chem. Soc.* **2008**, *130*, 1550−1551.
(34) Kubo, Y.; Minowa, Y.; Shoda, T.; Takeshita, K. *Tetrahedron Lett.* **2010**, *51*, 1600−1602.
(35) Wang, Y. W.; Descalzo, A. B.; Shen, Z.; You, X. Z.; Rurack, K. *Chem.—Eur. J.* **2010**, *16*, 2887−2903.
(36) Burghart, A.; Kim, H. J.; Welch, M. B.; Thoresen, L. H.; Reibenspies, J.; Burgess, K.; Bergstrom, F.; Johansson, L. B. A. *J. Org. Chem.* **1999**, *64*, 7813−7819.
(37) Rurack, K.; Kollmannsberger, M.; Daub, J. *New. J. Chem.* **2001**, *25*, 289−292.
(38) Bonardi, L.; Ulrich, G.; Ziessel, R. *Org. Lett.* **2008**, *10*, 2183−2186.
(39) Bellier, Q.; Pegaz, S.; Aronica, C.; Le Guennic, B.; Andraud, C.; Maury, O. *Org. Lett.* **2011**, *13*, 22−25.
(40) Goeb, S.; Ziessel, R. *Org. Lett.* **2007**, *9*, 737−740.
(41) Gresser, R.; Hummert, M.; Hartmann, H.; Leo, K.; Riede, M. *Chem.—Eur. J.* **2011**, *17*, 2939−2947.
(42) Gresser, R.; Hartmann, H.; Wrackmeyer, M.; Leo, K.; Riede, M. *Tetrahedron* **2011**, *67*, 7148−7155.
(43) Bellier, Q.; Dalier, F.; Jeanneau, E.; Maury, O.; Andraud, C. *New J. Chem.* **2012**, *36*, 768−773.
(44) Zhang, X.; Yu, H.; Xiao, Y. *J. Org. Chem.* **2012**, *77*, 669−673.
(45) Runge, E.; Gross, E. K. U. *Phys. Rev. Lett.* **1984**, *52*, 997−1000.
(46) Casida, M. E. In *Time-Dependent Density-Functional Response Theory for Molecules*; Chong, D. P., Ed.; World Scientific: Singapore, 1995; Vol. *1*, pp 155−192.
(47) Bauernschmitt, R.; Ahlrichs, R.; Hennrich, F. H.; Kappes, M. M. *J. Am. Chem. Soc.* **1998**, *120*, 5052−5059.
(48) Hirata, S.; Head-Gordon, M.; Bartlett, R. J. *J. Chem. Phys.* **1999**, *111*, 10774−10786.
(49) Adamo, C.; Barone, V. *Chem. Phys. Lett.* **2000**, *330*, 152−160.
(50) Cossi, M.; Barone, V. *J. Chem. Phys.* **2001**, *115*, 4708−4717.
(51) Dreuw, A.; Head-Gordon, M. *Chem. Rev.* **2005**, *105*, 4009−4037.
(52) Barone, V.; Polimeno, A. *Chem. Soc. Rev.* **2007**, *36*, 1724−1731.
(53) Fortrie, R.; Chermette, H. *J. Chem. Theory Comput.* **2007**, *3*, 852−859.
(54) Santoro, F.; Barone, V.; Improta, R. *J. Comput. Chem.* **2008**, *29*, 957−964.
(55) Goerigk, L.; Grimme, S. *J. Chem. Phys.* **2010**, *132*, 184103.
(56) Monari, A.; Assfeld, X.; Beley, M.; Gros, P. C. *J. Phys. Chem. A* **2011**, *115*, 3596−3603.
(57) Jacquemin, D.; Mennucci, B.; Adamo, C. *Phys. Chem. Chem. Phys.* **2011**, *13*, 16987−16998.
(58) Quartarolo, A. D.; Russo, N.; Sicilia, E. *Chem.—Eur. J.* **2006**, *12*, 6797−6803.
(59) Gao, L.; Senevirathna, W.; Sauvé, G. *Org. Lett.* **2011**, *13*, 5354−5357.
(60) Le Guennic, B.; Maury, O.; Jacquemin, D. *Phys. Chem. Chem. Phys.* **2012**, *14*, 157−164.
(61) To the best of our knowledge, this recent investigation by Zhang and co-workers,[44] where theoretical (gas-phase) fluorescence wavelengths are presented for three dyes is the only work where Aza-BODIPY excited-state geometries have been determined. However, the authors did not compute the vibrational spectra of the excited-state and, hence, had no access to the 0−0 energies nor the vibronic couplings.
(62) Send, R.; Valsson, O.; Filippi, C. *J. Chem. Theory Comput.* **2011**, *7*, 444−455.
(63) Jacquemin, D.; Zhao, Y.; Valero, R.; Adamo, C.; Ciofini, I.; Truhlar, D. G. *J. Chem. Theory Comput.* **2012**, *8*, 1255−1259.
(64) Frisch, M. J.; Trucks, G. W.; Schlegel, H. B.; Scuseria, G. E.; Robb, M. A.; Cheeseman, J. R.; Scalmani, G.; Barone, V.; Mennucci, B.; Petersson, G. A.; Nakatsuji, H.; Caricato, M.; Li, X.; Hratchian, H. P.; Izmaylov, A. F.; Bloino, J.; Zheng, G.; Sonnenberg, J. L.; Hada, M.; Ehara, M.; Toyota, K.; Fukuda, R.; Hasegawa, J.; Ishida, M.; Nakajima, T.; Honda, Y.; Kitao, O.; Nakai, H.; Vreven, T.; Montgomery, J. A., Jr.; Peralta, J. E.; Ogliaro, F.; Bearpark, M.; Heyd, J. J.; Brothers, E.; Kudin, K. N.; Staroverov, V. N.; Kobayashi, R.; Normand, J.; Raghavachari, K.; Rendell, A.; Burant, J. C.; Iyengar, S. S.; Tomasi, J.; Cossi, M.; Rega, N.; Millam, J. M.; Klene, M.; Knox, J. E.; Cross, J. B.; Bakken, V.; Adamo, C.; Jaramillo, J.; Gomperts, R.; Stratmann, R. E.; Yazyev, O.; Austin, A. J.; Cammi, R.; Pomelli, C.; Ochterski, J. W.; Martin, R. L.; Morokuma, K.; Zakrzewski, V. G.; Voth, G. A.; Salvador, P.; Dannenberg, J. J.; Dapprich, S.; Daniels, A. D.; Farkas, O.; Foresman, J. B.; Ortiz, J. V.; Cioslowski, J.; Fox, D. J. *Gaussian 09*, revision A.02; Gaussian Inc.: Wallingford CT, 2009.
(65) Furche, F.; Ahlrichs, R. *J. Chem. Phys.* **2002**, *117*, 7433−7447.
(66) Scalmani, G.; Frisch, M. J.; Mennucci, B.; Tomasi, J.; Cammi, R.; Barone, V. *J. Chem. Phys.* **2006**, *124*, 094107.
(67) Jacquemin, D.; Planchat, A.; Adamo, C.; Mennucci, B. *J. Chem. Theory Comput.* **2012**, *8*, 2359−2372.
(68) Becke, A. D. *J. Chem. Phys.* **1993**, *98*, 5648−5652.
(69) Stephens, P. J.; Devlin, F. J.; Chabalowski, C. F.; Frisch, M. J. *J. Phys. Chem.* **1994**, *98*, 11623−11627.
(70) Ernzerhof, M.; Scuseria, G. E. *J. Chem. Phys.* **1999**, *110*, 5029−5036.
(71) Adamo, C.; Barone, V. *J. Chem. Phys.* **1999**, *110*, 6158−6170.
(72) Adamo, C.; Scuseria, G. E.; Barone, V. *J. Chem. Phys.* **1999**, *111*, 2889−2899.
(73) Jacquemin, D.; Perpète, E. A.; Scuseria, G. E.; Ciofini, I.; Adamo, C. *J. Chem. Theory Comput.* **2008**, *4*, 123−135.
(74) Boese, A. D.; Martin, J. M. L. *J. Chem. Phys.* **2004**, *121*, 3405−3416.
(75) Zhao, Y.; Truhlar, D. G. *Theor. Chem. Acc.* **2008**, *120*, 215−241.
(76) Yanai, T.; Tew, D. P.; Handy, N. C. *Chem. Phys. Lett.* **2004**, *393*, 51−56.
(77) Chai, J. D.; Head-Gordon, M. *Phys. Chem. Chem. Phys.* **2008**, *10*, 6615−6620.
(78) Peach, M. J. G.; Benfield, P.; Helgaker, T.; Tozer, D. J. *J. Chem. Phys.* **2008**, *128*, 044118.
(79) Jacquemin, D.; Wathelet, V.; Perpète, E. A.; Adamo, C. *J. Chem. Theory Comput.* **2009**, *5*, 2420−2435.
(80) Mardirossian, N.; Parkhill, J. A.; Head-Gordon, M. *Phys. Chem. Chem. Phys.* **2011**, *13*, 19325−19337.
(81) Jacquemin, D.; Perpète, E. A.; Ciofini, I.; Adamo, C. *Theor. Chem. Acc.* **2011**, *128*, 127−136.
(82) Tomasi, J.; Mennucci, B.; Cammi, R. *Chem. Rev.* **2005**, *105*, 2999−3094.
(83) Cammi, R.; Mennucci, B. *J. Chem. Phys.* **1999**, *110*, 9877−9886.
(84) Caricato, M.; Mennucci, B.; Tomasi, J.; Ingrosso, F.; Cammi, R.; Corni, S.; Scalmani, G. *J. Chem. Phys.* **2006**, *124*, 124520.
(85) Improta, R.; Barone, V.; Santoro, F. *Angew. Chem., Int. Ed. Engl.* **2007**, *46*, 405−408.
(86) Santoro, F.; Improta, R.; Lami, A.; Bloino, J.; Barone, V. *J. Chem. Phys.* **2007**, *126*, 084509.
(87) Santoro, F.; Improta, R.; Lami, A.; Bloino, J.; Barone, V. *J. Chem. Phys.* **2007**, *126*, 184102.
(88) Santoro, F.; Lami, A.; Improta, R.; Bloino, J.; Barone, V. *J. Chem. Phys.* **2008**, *128*, 224311.
(89) Jacquemin, D.; Adamo, C. *Int. J. Quantum Chem.* **2012**, *112*, 2135−2141.
(90) Goerigk, L.; Moellmann, J.; Grimme, S. *Phys. Chem. Chem. Phys.* **2009**, *11*, 4611−4620.
(91) The SS correction is +0.121 eV with 6-31G(d) and +0.126 eV with 6-311+G(2d,p).

(92) Value computed in gas phase with counterpoise, CP, corrections for BSSE effects (gas phase model was used because PCM-CP corrections are not implemented in Gaussian09).
(93) Le Bahers, T.; Adamo, C.; Ciofini, I. *J. Chem. Theory Comput.* **2011**, *7*, 2498−2506.
(94) Jacquemin, D.; Le Bahers, T.; Adamo, C.; Ciofini, I. *Phys. Chem. Chem. Phys.* **2012**, *14*, 5383−5388; code available at Université de Nantes, http://www.sciences.univ-nantes.fr/CEISAM/erc/marches/ (accessed Aug 2012).
(95) B3LYP: 1.975 eV **15(a)** and 2.150 eV **15**($\mathbf{Hg^{2+}}$). BMK: 2.082 eV **15(a)** and 2.238 eV **15**($\mathbf{Hg^{2+}}$).
(96) Using the ZPVE correction obtained on the *naked* dye, **15**($\mathbf{Hg^{2+}}$).